

Testing the PDEM to Control the Precision of an IFSAR DEM

JOSE F. ZELASCO¹, KEVIN ENNIS[†], BARBARA SULPIS¹, JOSE LUIS FERNÁNDEZ AUSINAGA²

¹Facultad de Ingeniería - Universidad de Buenos Aires
Paseo Colón 850 – Ciudad de Buenos Aires
ARGENTINA

²Facultad de Ciencias Exactas – Universidad del Centro de la Pcia. de Bs. As.
Arroyo Seco, B7000 Tandil, Provincia de Buenos Aires
ARGENTINA

Abstract: The Perpendicular Distance Estimation Method (PDEM), a method to estimate the precision of a Digital Elevation Model (DEM), in “*Effectiveness of Geometric Quality Control Using a Distance Evaluation Method*” was tested assuming independent normal random for the vertical and horizontal error, considering isotropic this horizontal error. Here the PDEM is tested in the case of a DEM obtained by IFSAR technology, also, assuming independent normal random errors, but this time in three independent directions. Because vertical direction is correlated with one horizontal direction, -the range axis direction-, a rotation has to be done and so, three independent directions are obtained.

Keywords: GIS geometric accuracy assessment; IFSAR DEM geometric accuracy, Perpendicular Distance Evaluation Method (PDEM); IFSAR DEM quality evaluation.

Received: July 9, 2022. Revised: October 16, 2023. Accepted: November 18, 2023. Published: December 24, 2023.

1. Introduction and Description of Challenges.

A Digital Elevation Model (DEM) is a Digital Surface Model (DSM) of a terrain surface. It can be defined as a set of points, laid out on a regular square grid or on a triangular grid, where the altitudes are known in the vertices. The elevation anywhere else is obtained by interpolation. In the literature, often, the evaluation of the precision of a given DEM is obtained by “comparison” with a reference DEM considered “much more precise or exact” estimating the standard deviation of the discrepancies between them. To know the precision of different methods to obtain a DEM allows one to choose the method that has the best relation precision / price.

To carry out this comparison, two methods stand out in the literature: the measurement of vertical distances between the models and the comparison with benchmark points.

Zelasco2019 [17] describes these methods and establishes their limitations and drawbacks.

Briefly: the measurements of these vertical distances are affected by the slope of the reference DEM; and the corresponding points of these benchmarks may be subject to particular conditions or the benchmarks which have identifiable corresponding points are not a representative sample of the surface, Hirano et al. 2003 [8].

Also, in Zelasco2019 [17] the Perpendicular Distance Evaluation Method is formally presented and tested assuming independent normal random for the vertical

and horizontal error and considering isotropic the horizontal error.

The purpose of this article is to test the PDEM evaluating the geometric quality of a DEM obtained employing IFSAR technology. For the rest of the document, the given DEM will be referred to as the evaluated DEM (e-DEM). The reference DEM (r-DEM) is a real DEM of 100,000 points. The e-DEM is obtained by simulated errors from the r-DEM. Therefore, e-DEM errors are known. The PDEM evaluates the errors of the e-DEM by estimating the standard deviation in relation to the surface of the r-DEM. To test the PDEM it suffices to compare the estimated error values obtained by the PDEM with the known error values. As in Zelasco2019 [17], here, is assumed that the measurement errors are independent random variables with components in three orthogonal directions, and because the vertical direction is correlated with range axis a rotation has to be done given the beam axis, the azimuth axis and the axis normal to the previous two (y' ; the rotated range axis).

The rest of this paper is organized as follows: Section 2 provides the background of this study. Section 3 presents a brief description of the proposed method. Section 4 explains the error correlation of the e-DEM obtained by the IFSAR technology and the reformulation. Section 5 describes the experiments. Section 6 evaluates the results. Section. Finally, section 7 gives some concluding remarks regarding this study.

2. Background and Previous Problem Treatments.

The evaluation of a DEM error is an important topic, in the literature several attempts have been made for the evaluation of a DSM (e-DSM) error relating to a more precise reference DSM (r-DMS). Zelasco2019 [17] mention many previous works as Guptill and Morrison 1995 [5]; Harvey 1997 [6]; Laurini and Milleret-Raffort 1993 [10]; Ubeda and Servigne 1996 [15], and other several solutions concerning the DEM's quality proposed on Dunn et al. 1990 [2], Lester and Chrisman 1991 [9], etc. Also, analogous problems were studied for horizontal errors in maps in Abbas 1994 [1]; Grussenmeyer et al. 1994 [4]; Hottier 1996 [8]. They successfully use Hausdorff distance to evaluate the errors in maps, but this does not work in two dimensions in the cases when the components have different errors. Anyway, no solution to the simultaneous evaluation of vertical and horizontal errors is proposed.

The DEM Quality Assessment chapter in Maune 2001 [13], states that horizontal accuracy, although recognized as a part of DEM quality, is generally considered difficult to evaluate in the absence of an image coincident with the e-DEM (check points or benchmarks), or of clearly discernable surface features.

Zelasco 2019 [17] explains the lack, or at least scarcity, of work devoted to the horizontal accuracy of a DEM.

Zelasco et al. 2013 [16] is mostly a users' tutorial of the method.

In Zelasco 2019 [17] there is a formal presentation of the mechanics of the PDEM. The PDEM allows us to get statistical information about the horizontal and vertical standard deviations, only the perpendicular component of a point from the e-DEM to the r-DEM surface is required.

3. A brief description of the PDEM

Resuming Zelasco 2019 [17], the PDEM, unlike the vertical distance methods, produces vertical standard deviation results without a systematic error in the vertical direction and allows to obtain the horizontal variance under the condition of sufficient surface roughness.

The error is the vector function which denotes the discrepancy between both surfaces, and is defined for each point M_i and its homologous point P_i in the r-DEM. The points M_i define the e-DEM surface, but their homologous points P_i are not vertices of the r-DEM surface triangles. If they were, their

identification would be easy, and our problem would be trivial. However, we want to deal with the more common case in which the homologous points are not readily identifiable. The error vector is assumed to be the result of three stochastically independent components, e_x, e_y, e_z one in each of the basic axes of the x, y, z coordinate system. Notice that this error vector is not constrained to be vertical, nor necessarily orthogonal to any of the surfaces.

For each $P_i = [x_i, y_i, z_i]^T$, the error vector $\theta(x_i, y_i) = M_i(x_i, y_i) - P_i$, $i \in \{1, 2, \dots, n\}$ cannot usually be determined because of the difficulties in establishing the homologous point P_i . However, even if the homologous point P_i cannot be identified, the triangle $T_i \in$ r-DEM containing it, can usually be identified.

Fundamental property: An important property is that the projection of the error vector $\theta(x_i, y_i) = M_i(x_i, y_i) - P_i$ on a unitary vector N_i orthogonal to the surface $T_i \in$ r-DEM remains invariant if the point P_i is replaced by any other point $Q \in T_i$.

For the projection of the error vector on N_i the scalar product is

$$[M_i(x_i, y_i) - P_i] \cdot N_i = M_i - M'_i \quad (1)$$

where M'_i is the normal projection of M_i relative to the surface of the triangle T_i , the point of the triangle determined by the line normal to that triangle and which passes through M_i .

For any point Q belonging to the surface of the triangle T_i , we define a vector, which it will be called Q , the projection of the difference $M_i - Q$ on N coincides with the projection, on N , of $\theta(x_i, y_i) = M_i(x_i, y_i) - P_i$ (2)

Both projections are equal to $M_i - M'_i$. The fundamental property resulting from relation (1) is the reason for the choice of the name PDEM.

This relation implies that the length of the projection of the error vector may be computed

knowing only the triangle $T_i \in r\text{-DEM}$ that contains P_i , even without knowing the exact position of P_i .

Consequently, the variance of $M_i - M'_i$ is

$$\text{Var}\{M_i - M'_i\} = E\{|M_i - M'_i|^2\} = \sigma_{N_i}^2 = \sigma_x^2 \cdot \cos^2 \alpha_i + \sigma_y^2 \cdot \cos^2 \beta_i + \sigma_z^2 \cdot \cos^2 \gamma_i \quad (3)$$

where $\cos \alpha$, $\cos \beta$, $\cos \gamma$ are known, because they are the direction cosines of the normal unit vector, obtained from the data of the surface triangle $T_i \in r\text{-DEM}$, with

$$\cos^2 \alpha + \cos^2 \beta + \cos^2 \gamma = 1 \quad (4).$$

An estimator for this $\sigma_{N_i}^2$ is therefore the $M_i - M'_i$; if n observations were available, the estimator would be:

$$\frac{\sum_{j=1}^n |M_i - M'_i|^2}{n} \quad (5)$$

For different triangles we have different normal vectors, and different values of $\sigma_{N_i}^2$. Moreover, we have one observation for each, and one estimate for each. This gives us one relation for each. In these expressions, the coefficients: $\cos^2 \alpha_i$, $\cos^2 \beta_i$, $\cos^2 \gamma_i$ (4), are known, and σ_x^2 , σ_y^2 , σ_z^2 are unknown, and they are what we need to estimate. Our n expressions (4) give us an observation matrix, or design matrix

$$M = \begin{bmatrix} \cos^2 \alpha_1 & \cos^2 \beta_1 & \cos^2 \gamma_1 \\ \cos^2 \alpha_2 & \cos^2 \beta_2 & \cos^2 \gamma_2 \\ \dots & \dots & \dots \\ \cos^2 \alpha_i & \cos^2 \beta_i & \cos^2 \gamma_i \\ \dots & \dots & \dots \\ \cos^2 \alpha_n & \cos^2 \beta_n & \cos^2 \gamma_n \end{bmatrix} \quad (6)$$

The n expressions (4) allow us to establish n estimates for $\sigma_{N_i}^2$, which form a vector

$$L = \begin{bmatrix} \sigma_{N_1}^2 \\ \sigma_{N_2}^2 \\ \vdots \\ \sigma_{N_i}^2 \\ \vdots \\ \sigma_{N_n}^2 \end{bmatrix} \quad (7)$$

We may now estimate σ_x^2 , σ_y^2 , σ_z^2 as if they were the parameters of an ordinary linear regression of the output variable $\sigma_{N_i}^2$ as a linear function of the three variables $\cos^2 \alpha_i$, $\cos^2 \beta_i$, $\cos^2 \gamma_i$, given by (4). We have at our disposal n points, and the estimates may be obtained by the usual least squares regression method. We seek the values of σ_x^2 , σ_y^2 , σ_z^2 , which we may write as a vector

$$\sigma^2 = \begin{bmatrix} \sigma_x^2 \\ \sigma_y^2 \\ \sigma_z^2 \end{bmatrix} \quad (8)$$

and we seek to minimize the sum of squares of differences

$$\sum_{i=1}^n [\sigma_{N_i}^2 - (\sigma_x^2 \cdot \cos^2 \alpha_i + \sigma_y^2 \cdot \cos^2 \beta_i + \sigma_z^2 \cdot \cos^2 \gamma_i)]^2 = \sum_{i=1}^n \varepsilon_i^2 = (L - M \cdot \sigma^2)^T \cdot (L - M \cdot \sigma^2) \quad (9)$$

A complete discussion about the method is shown in Zelasco 2019 [19].

4. Error Correlation of the DEM Obtained by IFSAR: PDEM Reformulation.

The IFSAR geometry, see El-Taweel 2007 [3], Redadaa and Benslama, 2005 [14], Massonnet et al 1996 [11], and Massonnet and Feigl, 1995 [12] carries a correlation between y axes (range axis) and the z axis (Fig. 1).

It gets a diagonal covariance-matrix from a θ rotation around the x axis. This rotation joins the z' axis with the direction of the radar.

This hypothesis is justified by the formulas presented in El-Taweel 2007 [3] and Redadaa and Benslama, 2005 [14] as well as Massonnet et al, 1996 [11].

After the θ rotation, in the new referential, the x axis parallel to the trajectory of the satellite does not

change its position, the y' and z' directions correspond to the normal plane of the trajectory and the random variables in the three directions are not correlated.

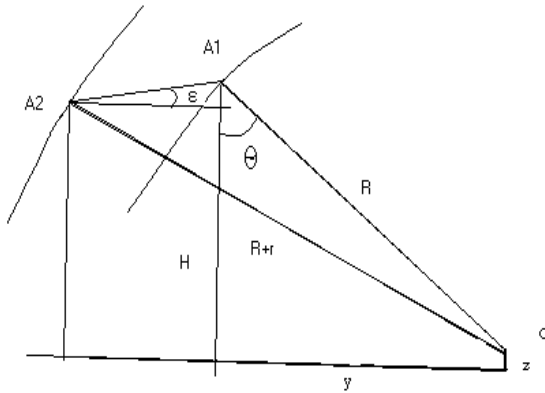


Figure 1

B is the base (distance between antennae $A1$ and $A2$), H is the height of the antennae $A1$ and R is the distance from $A1$ to the target C .

The value of z (height of the target) is given by: $z = H - R \cos \theta$, where H and R are known and $\cos \theta$ is incognito.

So: $(R + r)^2 = B^2 + R^2 + 2BR \cos \alpha$ where R , B , r (r is functional to the phase-difference and the wave length) are known.

In the triangle of vertices $A1$, $A2$ and C formed by the two antennae and the target, $R+r$ is the distance between $A2$ and C , the angle in $A1$ is α , and $\alpha = 90 + \theta - \varepsilon$ then,

$$\cos \alpha = \sin(\theta - \varepsilon).$$

Therefore:

$$\cos \theta = \cos \varepsilon \cdot \cos(\theta - \varepsilon) - \sin \varepsilon \sin(\theta - \varepsilon),$$

$$\text{and } \cos(\theta - \varepsilon) = (1 - \sin^2(\theta - \varepsilon))^{1/2}$$

Finally:

$$z = H - R \cdot \cos \theta \quad (10)$$

$$y = R \cdot \sin \theta \quad (11)$$

5. Description of the Experiment

The r-DEM is composed of a set of points that permits the construction of a net of K triangles. Each triangle T_k ($k=1, \dots, K$) belongs to a plane defined by a unitary vector η_k ($k=1, \dots, K$).

The following needs to be determined:

- - the coordinates of the center of each triangle expressed in the rotated reference system,

- a value of standard deviation σ_x , $\sigma_{y'}$ and $\sigma_{z'}$ for each direction in which the random variables are independent. Based on these values, random values that follow the normal law (noise) are determined. These new random values will be added to the coordinates of the center of mass of the triangles in the direction of the 3 axes expressed in this new reference. The new coordinate points constitute the (simulated) e-DEM.
- the coordinates of the normal unitary vector η_k to each triangle in the new referential
- the distance that separates each point from the e-DEM (simulated to evaluate), to the plane that contains the corresponding triangle
- the normal deviation of the points of the e-DEM in the directions of each coordinate of the rotated system: σ_x , $\sigma_{y'}$ and $\sigma_{z'}$.

Table 1 shows the results with triangles selected by considering the angle they have with the Z axis.

Results are presented, so that for each simulation they show:

- The value of σ used to produce noise on each axis,
- The PDEM estimation,
- The standard deviation of the estimation (over 20 times),
- The relative error (standard deviation/noise) of the estimations.

Fig. 2 shows the histograms of the PDEM, considering the angle, only with the Z axis.

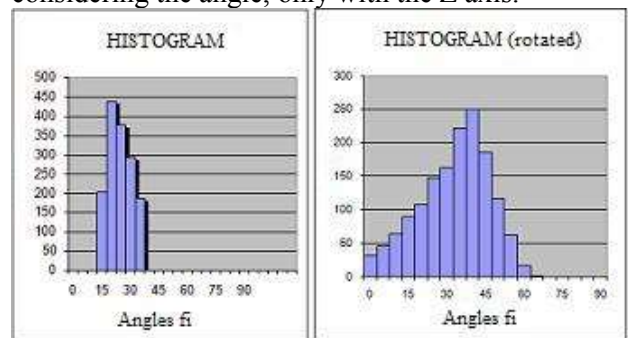


Figure 2: Previous Method PDEM Histogram.

Some results in Table 1 are not satisfactory for σ_x . To improve these results, we did other simulations (A, B, C, D, E, F) selecting triangles with respect to the 3 axes (not only to the Z axis)

For each simulation, we selected a different number of triangles with respect to each axis, indicating the triangle slope interval (FI_ALFA, FI_BETA o FI_GAMA) in relation to each axis (X , Y , and Z) respectively.

Test	Sigma			PDEM			Dev Es			E Relat.		
	En X	En Y	En Z	σ_X	σ_Y	σ_Z	σ_X	σ_Y	σ_Z	σ_X	σ_Y	σ_Z
1	10	15	20	---	15,3000	19,9400	---	1,3500	0,5700	---	0,0900	0,0300
2	10	20	15	13,4000	20,1700	14,9800	4,1200	0,9200	0,5400	0,4100	0,0500	0,0400
3	15	20	10	18,3000	20,0700	9,8900	1,7500	0,7300	0,5600	0,1200	0,0400	0,0600
4	15	10	20	18,1700	10,3000	19,9500	3,2900	1,6600	0,5600	0,2200	0,1700	0,0300
5	20	10	15	22,7600	10,1400	14,9500	1,8200	1,0300	0,4800	0,0900	0,1000	0,0300
6	20	15	10	22,6600	15,0400	9,9200	1,4400	0,6500	0,4700	0,0700	0,0400	0,0500
7	15	15	15	18,1600	15,1600	14,9400	2,2400	0,9100	0,4800	0,1500	0,0600	0,0300

Table 1

Simulation A produced the best results. For this simulation, 500 triangles were selected for each axis. The angle that forms the x axis with each of its 500 triangles does not exceed 60 degrees. The same criterion is taken into account for the y axis. It can be observed that in the direction of the x axis, the results are very satisfactory, except for the first two tests. Therefore, in the following section we only evaluate this simulation.

6. Evaluation of the Results

The average values in the three axes are given by:

$$\sigma_x = \left(\sum_n \sigma_{x_n} \right) / N;$$

$$\sigma_y = \left(\sum_n \sigma_{y_n} \right) / N;$$

$$\sigma_z = \left(\sum_n \sigma_{z_n} \right) / N$$

The standard deviation of σ_θ (variance-covariance matrix after rotation of a θ angle to nullify the correlation) is defined as: $\left\{ \sum_n (\sigma_n - \sigma_{(n)})^2 \right\} / N \}^{1/2}$

where $\sigma_{(n)}$ is the real value of the sample – very similar to the value used to produce the sampling of the errors (noise) – and σ_n is the value obtained by the PDEM.

We did several tests using different values to produce the noise (errors that produce the simulated e-DEM of study). This enabled us to study the behavior of the PDEM for different relations of noise in the axes. With the same values of noise, we performed each test over 20 times with different random values.

As it was said, six simulations were performed. The one with the best results (Simulation A), is obtained by selecting triangles related to the 3 axes in equal proportion (500 triangles in each case, it means a total of 1500) so that for the X and Y' axes, the triangle slope does not exceed 60 degrees and in the Z' axis it does not exceed 45 degrees.

For simulation A:

Table 2 shows the results with triangles selected by considering the angle they have with the three axes;

And again:

- The values of σ used to produce noise in each axis,
- The PDEM estimation,
- The standard deviation of the estimations (over 20 times),
- The relative error of the estimation.

Test	Sigma			PDEM			Dev Es			E Relat.		
	En X	En Y	En Z	σ_X	σ_Y	σ_Z	σ_X	σ_Y	σ_Z	σ_X	σ_Y	σ_Z
1	10	15	20	11,0320	15,3540	19,6250	2,6887	0,9756	0,8242	-0,0680	0,2874	-0,3473
2	10	20	15	11,5470	20,2411	14,5644	1,8159	0,9333	0,7273	0,3073	0,1522	-0,4148
3	15	20	10	16,3803	20,2059	9,4037	1,2016	0,8781	0,8360	0,3626	0,1170	-0,5825
4	15	10	20	15,7952	10,4864	19,6318	1,8417	1,0754	0,8217	0,0512	0,4419	-0,3405
5	20	10	15	20,6481	10,4367	14,5776	1,0889	0,9012	0,7433	0,1416	0,3823	-0,4016
6	20	15	10	20,8760	15,2700	9,4100	0,9535	0,7887	0,8511	0,2413	0,2033	-0,5761
7	15	15	15	16,0504	15,3063	14,5741	1,1955	0,8485	0,7152	0,2238	0,2390	-0,4051

Table 2: simulation A

Figure 3 shows the histograms obtained for the simulations A.

The histograms show how, after the rotation needed to nullify the correlation, the triangle slopes are modified. It is noteworthy that since the rotation is performed around the X axis, the first histogram remains unchanged.

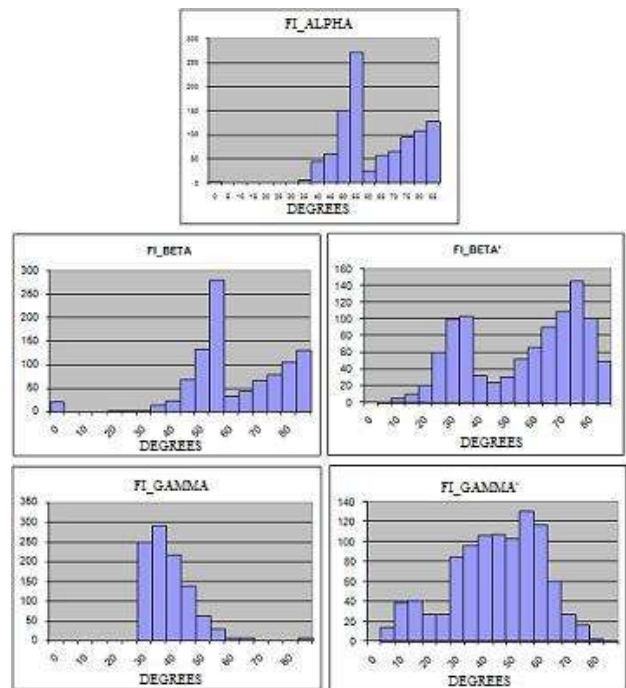


Figure 3: Reformulated Method PDEM Histogram (Simulation A).

The histograms show how, after the rotation needed to nullify the correlation, the triangle slopes are modified. It is noteworthy that since the rotation is

performed around the X axis, the first histogram remains unchanged.

7. Conclusions

In the case of DEM's obtained by IFSAR technology, the PDEM provides error estimation for the three not correlated directions: the beam axis, the azimuth axis and the axis normal to the previous two (y' ; the rotated range axis). As expected, the results are excellent in the direction of the beam axis. Since a rotation must be done to find the uncorrelated directions the unevenness of the surface artificially increases in the range axis direction therefore the error estimations are very good in the direction of the y' axis. The estimation error in the azimuth direction is compromised because it depends on enough irregular terrain conditions.

The PDEM provides a useful tool for evaluating the error of Digital Surface Models in the general case, as it was shown in previous works, and also when the DEM's are obtained by IFSAR technology.

Acknowledgement:

We thank Mr. Hugo RYCKEBOER for his comments and suggestions.

We extend our appreciation to Mr. Bernard Meyer for the real DEM used for testing the method.

References:

- [1] Abbas, Iyad., 1994. *Vector database and map error: Problems with spot control; an alternative method based on Hausdorff's distance: The linear control (Base de données vectorielles et erreur cartographique: problèmes posés par le contrôle ponctuel; une méthode alternative fondée sur la distance de Hausdorff: le contrôle linéaire)*. Thesis (PhD). Université Paris 7, France.
- [2] Dunn R., Harrison A. R. and White J. C., 1990. Positional accuracy and measurement error in digital databases of land use: An empirical study. *International Journal of Geographic Information Systems*, Vol 4 No 4, pp. 385-398.
- [3] El-Taweel, 2007. Enhanced Model for Generating 3-D Images from RADAR Interferometric Satellite Images. *WSEAS Transactions on Environment and Development*. Issue 3, Volume 3, ISSN: 1790-5079.
- [4] Grussenmeyer P., Hottier P. and Abbas I., 1994. The topographic control of a map or a database constituted by photogrammetric means (Le contrôle topographique d'une carte ou d'une base de données constituées par voie photogrammétrique). *Journal XYZ Association Française de Topographie*, No 59, pp. 39-45.
- [5] Guptill, S. C. and J. L. Morrison., 1995. *Elements of spatial data quality*. Oxford: Elsevier.
- [6] Harvey, F., *Quality Needs More Than Standards*. In: M.F. Goodchild, and R. Jeansoulin, eds. *Data Quality in Geographic Information: From Error to Uncertainty*. Paris: Hermes, 1998, 37-42.
- [7] Hirano, A., Welch R. and Lang H., 2003. Mapping from ASTER stereo image data : DEM validation and accuracy assessment. *ISPRS Journal of Photogrammetry and Remote Sensing*, No 57, pp. 356-370.
- [8] Hottier, P., 1996. Geometric quality of the planimetry. Punctual control and linear control. Dossier: The notion of precision in the GIS. (Qualité géométrique de la planimétrie. Contrôle ponctuel et contrôle linéaire. Dossier: La notion de précision dans le GIS). *Journal Géomètre, Ordre des Géomètres-Experts Français*, No 6, pp. 34-42.
- [9] Lester, M., and Chrisman, N., 1991. Not all slivers are skinny: a comparison of two methods for detecting positional error in categorical maps. *Proceedings of GIS/ LIS'91 Atlanta conference, October 28-November 1*, No 1, pp. 648-657.
- [10] Laurini, R., and Milleret-Raffort F. *Les bases de données en géomatique*. Paris: HERMES. 1993.
- [11] Massonnet D., Vadon H. and Rossi M., 1996. Reduction of the need for phase unwrapping in radar interferometry. *IEEE Transaction on Geosciences and Remote Sensing* No 34, pp. 489-497.
- [12] Massonnet D. and Feigl K. L., 1995. Radar interferometry and its applications to changes in the Earth surface. *Reviews of Geophysics* No 36, pp.441-500.
- [13] Maune, D. F., 2001. *Digital Elevation Model Technologies and Applications: The DEM Users Manual*. ASPRS
- [14] Redadaa S. and Benslam M., 2005. Topographic SAR Interferometry: A Geolocation Algorithm. *WSEAS Transactions on Systems*. Issue 12, Vol 4.
- [15] Ubeda, T. and Servigne, S., Geometric and Topological Consistency of Spatial Data. *Proceedings of the 1st International Conference on Geocomputation, Leeds, United Kingdom*, Sep. 17-19, pp. 830-842.

- [15] Zelasco J. F., Julien P., Porta G., Ennis K., Donayo J., 2013. PDEM Estimator for Digital Elevation Model: Utilities. *International Journal of Applied Mathematics and Informatics*, Vol 1 7, 24-31
- [16] Zelasco J. F., Donayo J., 2019. Effectiveness of Geometric Quality Control Using a Distance Evaluation Method. *International Journal of Image and Data Fusion*, Vol 10 No 4, pp. 263-279.

Contribution of Individual Authors to the Creation of a Scientific Article (Ghostwriting Policy)

The authors equally contributed in the present research, at all stages from the formulation of the problem to the final findings and solution.

Sources of Funding for Research Presented in a Scientific Article or Scientific Article Itself

No funding was received for conducting this study.

Conflict of Interest

The authors have no conflicts of interest to declare that are relevant to the content of this article.

Creative Commons Attribution License 4.0 (Attribution 4.0 International, CC BY 4.0)

This article is published under the terms of the Creative Commons Attribution License 4.0

https://creativecommons.org/licenses/by/4.0/deed.en_US